Transp Porous Med (2012) 94:437–459
DOI 10.1007/s11242-012-0013-1

Modeling the Chlorides Transport in Cementitious Materials By Periodic Homogenization

K. Bourbatache · O. Millet · A. Aït-Mokhtar · O. Amiri

Received: 17 April 2009 / Accepted: 17 April 2012 / Published online: 22 May 2012

Abstract In this work, we develop a macroscopic model for diffusion–migration of ionic species in saturated porous media, based on periodic homogenization. The prior application is chloride transport in cementitious materials. The dimensional analysis of Nernst–Planck equation lets appear dimensionless numbers characterizing the ionic transfer in porous media. Using experimental data, these dimensionless numbers are linked to the perturbation parameter ε. For a weak-imposed electrical field, or in natural diffusion, the asymptotic expansion of Nernst–Planck equation leads to a macroscopic model coupling diffusion and migration at the same order. The expression of the homogenized diffusion coefficient only involves the geometrical properties of the material microstructure. Then, parametric simulations are performed to compute the chloride diffusion coefficient through different complexity of the elementary cell to go on as close as possible to experimental diffusion coefficient of the two cement pastes tested.

Keywords Ionic transfer · Chlorides · Cementitious materials · Modeling · Periodic homogenization · Electrodiffusion test

1 Introduction

All reinforced concrete structures are subjected to aggressive environment, mainly carbon dioxide and chlorides. Chlorides come from marine environment in coastal regions or from de-icing salts in the other cold regions. The penetration of these aggressive agents through concrete cover leads to the corrosion of steel rebar in reinforced concrete (Poupard et al. 2003a,b). Important funds are spent for maintenance and repairs of degraded structures, the importance of which increases more and more. In European regions, the maintenance costs reach in the beginning of the century about € 5 billions per year (Klinghoffer et al. 2000). Therefore, many researches have focused on this topic, and on getting the chloride diffusion

K. Bourbatache · O. Millet (✉) · A. Aït-Mokhtar · O. Amiri
La Rochelle University, LaSIE, Avenue Michel Crépeau, 17000 La Rochelle, France
e-mail: olivier.millet@univ-lr.fr

coefficient by applying Fick's laws or by developing accelerated tests in laboratories (Amiri et al. 1997). Later, other researches proved that Fick's laws seem not to be valid because of three main reasons:

- The ionic transport is different from the molecular or particle transport. In ionic transport, there are electrochemical interactions between the different ions contained in the pore solution and a global approach of studying the movement of all species contained in the pore solution must be undertaken to correctly describe the chloride transport (Amiri et al. 2001a,b).
- The cementitious materials are strongly heterogeneous because of the cement hydration processes with the presence of aggregates (sand and gravels) in case of concrete. The different hydrates formed are with different geometries, shapes, and sizes. They lead to complex microstructure geometry. Therefore, approaches considering the material homogeneous do not allow accurately to describe the transfer processes within the material. With Fick's approach, the cementitious material seems to be a black box, where only boundary and initial conditions around the specimen are monitored (Amiri et al. 1997).
- There are chemical and electrochemical interactions at the interface between the ionic pore solution and the solid phase, mainly the cement matrix (Friedmann et al. 2004).

Therefore, to investigate the mechanisms involved during the ionic diffusion through cement-based materials, it seems necessary to undertake modeling and adequate experimental studies accounting for the phenomena cited above. Therefore, we propose in this work to compute a macroscopic predictive modeling of ionic transfer in cementitious porous materials, taking into account the microstructure and the multi-scale properties of such materials.

Homogenization techniques, which enable to obtain macroscopic or homogenized equations from the behavior at the microscopic level, have been developed since the 1970s. The first works, based on a direct volume averaging of local or microscopic equations, have been developed in Whitaker (1983), Whitaker et al. (1988). The application of this volume averaging technique has been essentially limited to linear transfer equations (Whitaker et al. 1988; Quintard and Whitaker 1993). For nonlinear equations, and in particular for the nonlinear Nernst–Planck Poisson system[1] considered in this paper, its application encountered some difficulties. In parallel, from the end of the 1970s, periodic homogenization techniques, based on the double scale asymptotic expansion analysis, have been developed (Bensoussan et al. 1978; Sanchez Palencia 1980). They have already been applied successfully to transport laws in porous media and in particular to Fick's diffusion (Auriault and Lewandowska 1996), and even for nonlinear diffusion (Auriault and Lewandowska 1997) or nonlinear flows (Skjetne and Auriault 1999). It has been also extended to a coupling with electrical potential gradients by quasi-static Maxwell and Navier–Stokes equations (Auriault and Strzelecki 1981), or to an alternative microscale bulk formulation for expansive clays (Moyne and Murad 2003, 2006).

In this work, we propose to apply the periodic homogenization technique to the nonlinear Nernst–Planck–Poisson system. Given the representative elementary volume (REV) of a cement-based material, we will consider an isotropic transfer in the fluid phase of the material. In a first step, we consider the case of cement pastes with 0.5 and 0.7 water/cement ratios. For this kind of cement-based materials, the main porosity is a capillary porosity, where the electrical double layer effect could be neglected. Therefore, the experimental validation of the proposed approach is performed on these two cement pastes, for which the homogenization process at the scale of capillary porosity is relevant. The paper begins with

[1] Which governs the ionic transfer in porous materials.

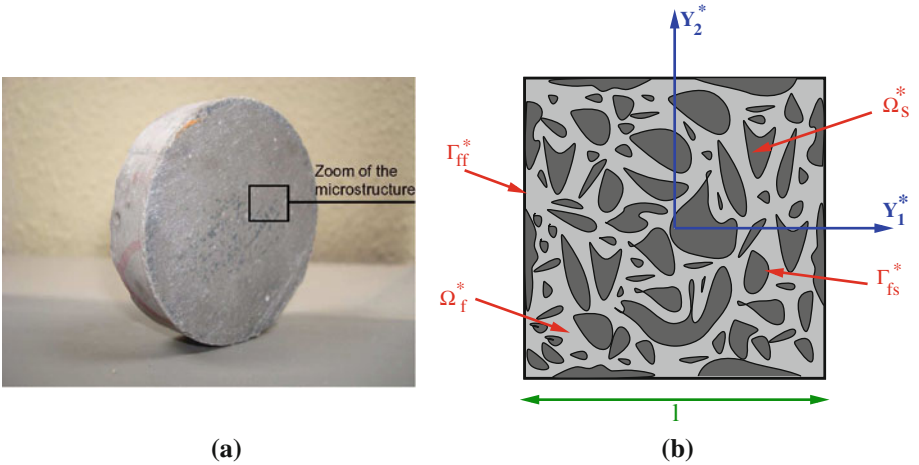

Fig. 1 Modelling of the material microstructure with a periodic elementary cell. **a** The sample of cement paste considered. **b** Example of periodic microstructure for saturated porous materials

the theoretical background and the modeling basis. After that, the experimental validation on cement pastes is carried out. Finally, numerical simulations for computing homogenized transfer properties, mainly the calculation of macroscopic diffusion coefficient are presented. These simulations were performed by considering different geometries of elementary cells, which integrate tortuosity and constrictivity factors of the materials porous network.

2 Coupled Transport Equations in Saturated Porous Media

The medium considered is a heterogeneous saturated porous material, the microstructure of which contains two phases: a solid phase of cement paste and eventually aggregates, in case of mortars or concrete Ω_{s*}, and a liquid phase Ω_{f*} (see Fig. 1). We note Γ_{fs*} the boundary between the solid and the liquid phases, and V^* the convection velocity of the fluid assumed to be incompressible. The chemical interactions between the liquid and the solid phases are neglected.

In what follows, we will index by a star (*) all dimensional variables. The variables without a star are dimensionless. Moreover, grad*, div*, and Δ^* will denote the three-dimensional gradient, divergence, and Laplacian with respect to the dimensional variables, respectively.

The diffusion in the fluid phase is described by Nernst–Planck equation[2] coupled with Poisson equation characterizing the electrical fields accelerating the ionic transfer. Nernst–Planck–Poisson system is generally written for an isotropic diffusivity assumed in the fluid phase (Amiri et al. 2001a; Bard and Faulkner 2001; Lipkowski and Ross 1994; Newman and Thomas-Alyea 2004; Samson et al. 1999):

$$\frac{\partial^* C_k^*}{\partial t^*} + \mathrm{div}^*\left(-D_k^* \mathrm{grad} C_k^* - \frac{F}{RT} D_k^* \mathrm{grad}^* \Psi^* Z_k C_k^* + V^* C_k^*\right) = 0 \text{ in } \Omega_{f*} \qquad (1)$$

where C_k^* denotes the concentration of the ionic species k of valence Z_k, D_k^* its molecular diffusion coefficient in the liquid phase (the pore solution for cementitious materials),

[2] This equation corresponds to the mass conservation for the ionic species of concentration C_{k*} diffusing in the liquid phase.

$E^* = -\text{grad}^*\Psi^*$ the electrical field in the solution, F and R, respectively, the Faraday and the ideal gas constant, T the temperature of the fluid, and V^* the convection velocity of the fluid.

The Poisson equation characterizing the potential Ψ^* writes

$$\Delta^*\Psi^* = -\frac{\rho^*}{\varepsilon_v} \text{ in } \Omega_{f^*} \tag{2}$$

where $\varepsilon_v = \varepsilon_0\varepsilon_f$ denotes the dielectric constant of the fluid phase. The electrical charge density ρ^* is defined by

$$\rho^* = \sum_{k=1}^{N} F Z_k C_k^* \tag{3}$$

where N denotes the number of ionic species involved in the transfer.

The solid phase in cementitious saturated porous materials can be considered as non conductive with respect to the fluid one. The boundary conditions associated with Eqs. (1) and (2) write:

$$D_k^*(\text{grad}^* C_k^* + \frac{F Z_k}{RT}\text{grad}^*\Psi^*) \cdot n = 0 \text{ on } \Gamma_{sf}^* \tag{4}$$

and

$$\text{grad}^*\Psi^* \cdot n = 0 \text{ on } \Gamma_{sf}^* \tag{5}$$

where n denotes the external unit normal to the solid domain Ω_{s^*}. These Neumann boundary conditions represent the non penetration of the ionic species and of the electrical field in the solid phase Ω_{s^*} (the solid phase is considered non conductive).

Moreover, considering the homogeneous boundary condition (5) is equivalent to neglect the electrocapillary adsorption at the liquid–solid interface, which constitutes the electrical double layer. This is coherent with the homogenization procedure which will be performed at the scale of the capillary porosity of the cement pastes considered, where the characteristic length of the elementary cell is much larger than the Debye's length so that the double layers effect can be neglected in a first step of our researches.

Equation (1) must be completed with Stokes equation and the incompressibility condition for the fluid:

$$\text{div}^* V^* = 0 \text{ in } \Omega_f^* \tag{6}$$

However, in saturated cementitious materials the convection velocities are very weak and the convection phenomena are negligible (see Sect. 3.3). Thus, in our study, the Stokes equation will not be developed. It would lead after homogenization to the classical Darcy equation at the macroscopic scale (Sanchez Palencia 1980; Auriault and Lewandowska 1996).

3 The Periodic Homogenization Procedure

The periodic homogenization technique relies on the assumption that the microstructure of the material can be considered as periodical, i.e., as the repetition of an elementary cell the size and complexity of which depend on the real microstructure. In general, even if this assumption is never verified exactly, it constitutes a good approximation of the reality if the

elementary cell is sufficiently complex and constitutes a kind of a REV. Once this assumption admitted, the fields involved (concentration, electrical field,…) and their derivatives must be considered as periodical on the cell boundary so that the problem is mathematically consistent.

3.1 Description of the Periodic Microstructure

Let us consider at the macroscopic scale that the material studied (here a cement paste on Fig. 1a) occupies the domain S^* of the three-dimensional space $\mathbb{R}^3$, with a characteristic length L. At the macroscopic level, a current point of S^* will be noted $x^* = (x_1^*,\ x_2^*,\ x_3^*)$.

We assume that the material S^* has a periodic microstructure, or equivalently is constituted of the periodic repetition of an elementary cell $\Omega^* = \Omega_{\mathrm{f}}^* \cup \Omega_{\mathrm{s}}^*$ composed of a fluid phase Ω_{f}^* and of a solid phase Ω_{s}^* (Fig. 1). The boundary Γ^* of Ω_{f}^* is composed of the inner boundary Γ_{fs}^* between the fluid and the solid phases, and of the part Γ_{ff}^* between the fluid phases of two neighbouring cells. At the microscopic level, a current point of the elementary cell Ω^* is noted $y^* = (y_1^*,\ y_2^*,\ y_3^*)$.

Moreover, the size l of the elementary cell Ω^* is assumed to be very small with respect to the dimension L of the material. This is a condition of the homogenizability of the problem. Thus, the aspect ratio ε satisfies

$$\varepsilon = \frac{l}{L} \ll 1$$

Finally, problem (1)–(5) written at the microscale level (at the scale of the elementary cell) must be completed with boundary conditions at the macroscale level or equivalently at the scale of the material S^*. In this work, we consider that the concentrations C_k^* of the ionic species are given on the boundary ∂S^* of the structure S^*, and that the electrical field E^* may be imposed on ∂S^* if we are not in natural diffusion. Moreover, the initial conditions at $t^* = 0$ are assumed to be given by the experimental data (see experimental procedure described in Sect. 3.3).

3.2 Dimensional Analysis of Equations

The dimensional analysis of Eqs. (1)–(6) is similar to that developed in Millet et al. (2008). Following the reasoning of Auriault and Lewandowska (1996), Hamdouni and Millet (2003), Millet et al. (1997, 2001), we define dimensionless physical data and dimensionless unknowns of the problem:

$$y = \frac{y^*}{l},\quad x = \frac{x^*}{L},\quad t = \frac{t^*}{t_{\mathrm{r}}},\quad D_k = \frac{D_k^*}{D_{\mathrm{r}}},\quad C_k = \frac{C_k^*}{C_{\mathrm{r}}},\quad \Psi = \frac{\Psi^*}{\Psi_{\mathrm{r}}},\quad V = \frac{V^*}{V_{\mathrm{r}}} \tag{7}$$

where the variables indexed by r are the reference ones and the new variables which appear (without a star) are dimensionless. The microscopic length l will be used to normalize the spatial differential operators.

Introducing the dimensionless variables previously defined in Eqs. (1) and (2), we obtain a new dimensionless problem posed in Ω_f:

$$\tau \frac{\partial C_k}{\partial t} + \mathrm{div}\Big(-D_k \mathrm{grad} C_k - \mathscr{R} D_k \mathrm{grad}\Psi\, Z_k C_k + \mathscr{P} V C_k\Big) = 0 \text{ in } \Omega_{\mathrm{f}} \tag{8}$$

$$\mathscr{A}\,\Delta\Psi = -\rho \text{ in } \Omega_{\mathrm{f}} \tag{9}$$

where grad, div, and Δ denote respectively the three-dimensional gradient, divergence, and Laplacian with respect to non-dimensional variables, and where we set $\rho = \sum_{k=1}^{N} Z_k C_k$. The associated dimensionless boundary conditions become

$$D_k(\mathrm{grad}C_k + \mathscr{R}\mathrm{grad}\Psi Z_k C_k)\cdot n = 0 \text{ on } \Gamma_{\mathrm{sf}} \tag{10}$$

$$(\mathrm{grad}\Psi)\cdot n = 0 \text{ on } \Gamma_{\mathrm{sf}} \tag{11}$$

Hence, the dimensional analysis of Nernst–Planck and Poisson equations naturally leads to dimensionless numbers characterizing the diffusion–migration–convection problem:

$$\mathscr{P} = \frac{V_{\mathrm{r}} l}{D_r}, \quad \tau = \frac{l^2}{D_{\mathrm{r}} t_{\mathrm{r}}}, \quad \mathscr{R} = \frac{\Psi_{\mathrm{r}} F}{RT}, \quad \mathscr{A} = \frac{\Psi_{\mathrm{r}} \varepsilon_{\mathrm{v}}}{F l^2 C_{\mathrm{r}}}. \tag{12}$$

The first one is the classical Peclet number, ratio of the convective to the diffusive effects. The dimensional number $\tau = \dfrac{l^2}{D_{\mathrm{r}} t_{\mathrm{r}}}$ represents the ratio of the characteristic time $\frac{l^2}{D_{\mathrm{r}}}$ of the molecular diffusion at the microscale to the characteristic time at the macroscale t_{r} defined in (7). It is a small parameter of the problem. The dimensionless number $\mathscr{R} = \dfrac{\Psi_{\mathrm{r}} F}{RT}$ depends directly on the applied electrical potential and can take important values. Finally, $\mathscr{A} = \dfrac{\Psi_{\mathrm{r}} \varepsilon_{\mathrm{v}}}{F l^2 C_{\mathrm{r}}}$ couples the effects of the applied electrical potential and the concentrations of the ionic species in the pore solution of the material.

3.3 Reduction to a One-Scale Problem

To apply the periodic homogenization procedure to the problem of ionic transport considered, we must reduce first our dimensionless problem to a one-scale problem. To do this, $\varepsilon = \dfrac{l}{L}$ is chosen as the reference perturbation parameter. Then, the other dimensionless numbers, which are given data for the cement pastes studied (see Sect. 5 of this paper), are linked to ε.

- First, the determination of the aspect ratio $\varepsilon = \dfrac{l}{L}$ of the homogenization problem comes directly from the results of the mercury intrusion porosimetry (MIP). For the cement paste, we will consider a characteristic length of the elementary cell[3] $l = 10\,\mu$m. Therefore, we have

$$\varepsilon = \frac{l}{L} = 10^{-3}$$

- We focus in this paper on diffusion–migration of chlorides through cements pastes, the diffusion coefficient of which in infinite dilution in water at 25°C is $10^{-9}\,\mathrm{m^2\,s^{-1}}$ so that we consider here that $D_{\mathrm{r}} = 10^{-9}\,\mathrm{m^2\,s^{-1}}$. Moreover, in the chlorides migration tests developed (see Sect. 5), the chlorides concentration involved is $0.5\,\mathrm{mol\,l^{-1}}$ (equivalent to seawater concentration) so that we consider that the reference concentration is $C_{\mathrm{r}} = 0.5\,\mathrm{mol\,l^{-1}}$.
- On the other hand, the convection velocity V_{r} of the fluid in the process of ionic transfer studied is very slow. It is of the order of $V_{\mathrm{r}} = 10^{-13}\mathrm{m\,s^{-1}}$ (or equivalently 1 mm per week) so that we have $\mathscr{P} = O(\varepsilon^2)$.

[3] For the homogenization process to be consistent, the mean pore radii must be small with respect to the size l of the elementary cell.

- Finally, in the case of a natural diffusion or a weak applied electrical field, the reference time representative of the diffusion process is rather long; it could be of the order of several weeks (or even several months) so that we shall consider $t_r = 10^6$ s.

Therefore, in the case of a weak applied electrical field and a weak convection velocity, the orders of magnitude of the dimensionless numbers considered stands:

$$\mathscr{R} = O(1), \quad \mathscr{A} = O(\varepsilon^2), \quad \tau = O(\varepsilon^2) \quad \text{and} \quad \mathscr{P} = O(\varepsilon^2) \tag{13}$$

4 The Macroscopic Diffusion–Migration Model for a Weak Applied Electrical Field or a Natural Diffusion

For the order of magnitude of the dimensional numbers considered in (13), the non-dimensional equations (8)–(9) reduce to:

$$\varepsilon^2 \frac{\partial C_k}{\partial t} + \operatorname{div}\Big(-D_k \operatorname{grad} C_k - D_k \operatorname{grad}\Psi\, Z_k C_k + \varepsilon^2 \mathscr{P} V C_k\Big) = 0 \tag{14}$$

$$\varepsilon^2 \Delta \Psi = -\rho \tag{15}$$

with the associated boundary conditions:

$$D_k(\operatorname{grad} C_k + Z_k C_k \operatorname{grad}\Psi) \cdot n = 0 \text{ on } \Gamma_{sf} \tag{16}$$

$$(\operatorname{grad}\Psi) \cdot n = 0 \text{ on } \Gamma_{sf} \tag{17}$$

4.1 Asymptotic Expansion of Equations

The classical procedure of periodic homogenization (Bensoussan et al. 1978; Sanchez Palencia 1980) leads to search the unknowns C_k, Ψ, V of the problem as functions depending on the macroscopic variable x, on the microscopic variable y, and on the time t, considered as separate variables. This is justified because of the separation of scales ($\varepsilon \ll 1$). Moreover, the unknowns C_k, Ψ, V of the problem are postulated to admit a formal expansion with respect to ε:

$$\begin{aligned} C_k &= C_k^0(x, y, t) + \varepsilon C_k^1(x, y, t) + \varepsilon^2 C_k^2(x, y, t) + \cdots \\ \Psi &= \Psi^0(x, y, t) + \varepsilon \Psi^1(x, y, t) + \varepsilon^2 \Psi^2(x, y, t) + \cdots \\ V &= V^0(x, y, t) + \varepsilon V^1(x, y, t) + \varepsilon^2 V^2(x, y, t) + \cdots \end{aligned} \tag{18}$$

Finally, as $\rho = \sum_{k=1}^{N} Z_k C_k$, it admits as well an expansion will respect to ε, similar to (18).

An important point concerns the calculation of the derivative operators grad and div with respect to the functions $C_k^i(x, y, t)$, $\Psi^i(x, y, t)$, $V^i(x, y, t)$, for $i \in \mathbb{N}^*$. As these functions depend on the *independent* space variables x and y, the derivatives must be considered as composed derivative of several variable functions. In other terms, according to the separation of variables with respect to the scales L and $l = \varepsilon L$, and to the dimensional analysis performed, we have

$$\operatorname{grad} = \frac{\partial}{\partial y} + \varepsilon \frac{\partial}{\partial x}; \quad \operatorname{div} = \operatorname{div}_y + \varepsilon \operatorname{div}_x; \quad \Delta = \Delta_y + 2\varepsilon \frac{\partial^2}{\partial x \partial y} + \varepsilon^2 \Delta_x \tag{19}$$

where $\frac{\partial}{\partial y}$, div_y, and Δ_y denote respectively the gradient, the divergence, and the Laplacian with respect to the local variable y, $\frac{\partial}{\partial x}$, div_x, and Δ_x, respectively, the gradient, the divergence, and the Laplacian with respect to the macroscopic variable x.

Replacing C_k, Ψ, and V by their expansions (18) in the dimensionless equilibrium equations (14)–(17) and equating to zero the factors of successive powers of ε, we obtain the coupled problems $\mathscr{P}_0$, $\mathscr{P}_1$, …, corresponding respectively to the cancellation of the factors of ε^0, ε^1, …

4.2 The Macroscopic Diffusion–Migration Model

Result 1 *For orders of the dimensionless numbers such as* $\mathscr{R} = O(1)$, $\mathscr{A} = O(\varepsilon^2)$, $\tau = O(\varepsilon^2)$, *and* $\mathscr{P} = O(\varepsilon^2)$, *the leading terms* C_k^0 *of the expansion of* C_k *satisfy the electroneutrality assumption at the first order*:

$$\rho^0 = \sum_{k=1}^{N} Z_k C_k^0 = 0 \tag{20}$$

Moreover, the macroscopic concentration C_k^0 *and potential* Ψ^0 *at the scale of the material are solution of the homogenized diffusion–migration model*:

$$\varphi \frac{\partial C_k^0}{\partial t} - \mathrm{div}_x \left(\mathbf{D_k^{hom}} \frac{\partial C_k^0}{\partial x} + \mathbf{D_k^{hom}} \frac{\partial \Psi^0}{\partial x} Z_k C_k^0 \right) = 0 \tag{21}$$

The homogenized diffusion tensor $\mathbf{D_k^{hom}}$ *is given by*

$$\mathbf{D_k^{hom}} = \frac{1}{|\Omega|} \int_{\Omega_f} D_k \left(I + \overline{\frac{\partial \chi}{\partial y}} \right) \mathrm{d}\Omega \tag{22}$$

where the vector $\chi(y)$ *is the solution of the boundary problem*:

$$\begin{cases} \mathrm{div}_y \left(D_k \left(I + \overline{\frac{\partial \chi}{\partial y}} \right) \right) = 0 \text{ in } \Omega_\mathrm{f} \\ D_k \left(I + \frac{\partial \chi}{\partial y} \right) \cdot n = 0 \text{ on } \Gamma_\mathrm{sf} \end{cases} \tag{23}$$

Demonstration : *The demonstration of this result is split into four steps from* (i) *to* (iv)

(i) *The electroneutrality assumption*
The cancellation of the factor of ε^0 in Poisson equation (15) leads straightforward at order zero to the electroneutrality condition:

$$\rho^0 = \sum_{k=1}^{N} Z_k C_k^0 = 0 \tag{24}$$

Thus, for the orders of the dimensional numbers considered (corresponding to a weak imposed electrical field or a natural diffusion), the electroneutrality assumption is justified at the first order from the asymptotic expansion of equations.

(ii) *The fields* C_k^0 *and* ψ^0 *do not depend on* y

The cancellation of the factor of ε^0 in Nernst–Planck equations (14) and (16), leads to problem $\mathscr{P}_0$:

$$\mathrm{div}_y\left(-D_k \mathrm{grad}_y C_k^0 - D_k \mathrm{grad}_y \Psi^0 Z_k C_k^0\right) = 0 \tag{25}$$

with the associated boundary conditions:

$$D_k(\mathrm{grad}_y C_k^0 + Z_k C_k^0 \mathrm{grad}_y \Psi^0) \cdot n = 0 \text{ on } \Gamma_{\mathrm{sf}} \tag{26}$$

To prove that the fields C_k^0 and Ψ^0 do not depend on y at the leading order, let us write the weak formulation associated to Eq. (25). To do this, let us multiply (25) by a test function $v_k \in V$, where V denotes the space of test functions without entering into mathematical considerations[4]. Moreover, for the simplicity of the proof, let us consider that the diffusion coefficient D_k is constant and does not depend on y (it is the case in the diffusion–migration problems that will be considered in Sect. 5). Then, an integration upon the fluid domain Ω_{f}, by the divergence theorem, boundary conditions (26), and the periodicity of the fields on Γ_{ff}, leads to

$$\int_{\Omega_{\mathrm{f}}} \mathrm{grad}_y C_k^0 \cdot \mathrm{grad}_y v_k \mathrm{d}y + \int_{\Omega_{\mathrm{f}}} Z_k C_k^0 \mathrm{grad}_y \Psi^0 \cdot \mathrm{grad}_y v_k \mathrm{d}y = 0 \quad v_k \in V \tag{27}$$

where the dot denotes the scalar product of $\mathbb{R}^3$. Hence, choosing $v_k = \psi^0$ in (27), it stands:

$$\int_{\Omega_{\mathrm{f}}} \mathrm{grad}_y C_k^0 \cdot \mathrm{grad}_y \psi^0 \mathrm{d}y + \int_{\Omega_{\mathrm{f}}} Z_k C_k^0 \|\mathrm{grad}_y \Psi^0\|^2 \mathrm{d}y = 0 \tag{28}$$

where $\|u\|^2$ denotes the classical norm of vector u in $\mathbb{R}^3$. Now, let us multiply (28) by Z_k for each k and sum the equations obtained. It leads to

$$\int_{\Omega_{\mathrm{f}}} \mathrm{grad}_y \left(\sum_{k=1}^{N} Z_k C_k^0\right) \cdot \mathrm{grad}_y \psi^0 \mathrm{d}y + \int_{\Omega_{\mathrm{f}}} \left(\sum_{k=1}^{N} Z_k^2 C_k^0\right) \|\mathrm{grad}_y \Psi^0\|^2 \mathrm{d}y = 0 \tag{29}$$

Using the electroneutrality condition at order zero (Eq. (24)), the first term of Eq. (29) vanishes and we finally obtain

$$\int_{\Omega_{\mathrm{f}}} \left(\sum_{k=1}^{N} Z_k^2 C_k^0\right) \|\mathrm{grad}_y \Psi^0\|^2 \mathrm{d}y = 0 \tag{30}$$

As all the concentrations C_k are by definition positive or null, this stays valid at the leading order and we have $C_k^0 \geq 0 \; \forall k$. Moreover, at least one of the concentration is different from zero, for the problem to be physically consistent so that there exists k such as $C_k^0 \neq 0$, and by consequence $\sum_{k=1}^{N} Z_k^2 C_k^0 > 0$. Therefore, Eq. (30) implies that $\|\mathrm{grad}_y \Psi^0\|^2 = 0$ or equivalently:

$$\Psi^0 = \Psi^0(x, t) \tag{31}$$

[4] In fact, we have here $V = H^1(\Omega_{\mathrm{f}})$ where $H^1(\Omega_{\mathrm{f}})$ denotes the classical Hilbert space of order one.

To finish, let us come back to the weak formulation (27). Accounting for (31), choosing $v_k = C_k^0$, it reduces to:

$$\int_{\Omega_{PF}} \|\text{grad}_y C_k^0\|^2 \text{d}y = 0 \tag{32}$$

which implies that $\text{grad}_y C_k^0 = 0$ or equivalently:

$$C_k^0 = C_k^0(x,\, t) \tag{33}$$

Hence, we have proved that at the leading order, the fields C_k^0 and Ψ^0 do not depend on the microscopic variable y.

(iii) *Determination of* Ψ^1 *and* C_k^1

According to (31) and (33), the cancellation of the factor of ε^1 in Nernst–Planck equations leads to the problem $\mathscr{P}_1$ which reduces to[5]:

$$\text{div}_y\left(D_k\left(\frac{\partial C_k^0}{\partial x} + \frac{\partial C_k^1}{\partial y}\right) + D_k\left(\frac{\partial \Psi^0}{\partial x} + \frac{\partial \Psi^1}{\partial y}\right) Z_k C_k^0\right) = 0 \text{ in } \Omega_{\text{f}} \tag{34}$$

$$\left(D_k\left(\frac{\partial C_k^0}{\partial x} + \frac{\partial C_k^1}{\partial y}\right) + D_k\left(\frac{\partial \Psi^0}{\partial x} + \frac{\partial \Psi^1}{\partial y}\right) Z_k C_k^0\right) \cdot n = 0 \text{ on } \Gamma_{\text{sf}} \tag{35}$$

Let us write Eqs. (34) and (35) on the following form:

$$\text{div}_y\left(D_k\left(\frac{\partial C_k^1}{\partial y} + \frac{\partial \Psi^1}{\partial y} Z_k C_k^0\right)\right) = -\text{div}_y\left(D_k\left(\frac{\partial C_k^0}{\partial x} + \frac{\partial \Psi^0}{\partial x} Z_k C_k^0\right)\right)$$

$$\left(D_k\left(\frac{\partial C_k^1}{\partial y} + \frac{\partial \Psi^1}{\partial y} Z_k C_k^0\right)\right) \cdot n = \left(-D_k\left(\frac{\partial C_k^0}{\partial x} + \frac{\partial \Psi^0}{\partial x} Z_k C_k^0\right)\right) \cdot n$$

and consider that the right hand side involving $C_k^0(x,\, t)$ and $\Psi^0(x,\, t)$ is known. The left hand side is elliptic with respect to $C_k^1 + \Psi^1 Z_k C_k^0$ and we can prove that we have

$$C_k^1 + \Psi^1 Z_k C_k^0 = \overline{A}^1(x,\, t) + \chi(y) \cdot \left(\frac{\partial C_k^0}{\partial x} + \frac{\partial \Psi^0}{\partial x} Z_k C_k^0\right) \text{ in } \Omega_{\text{f}} \tag{36}$$

where χ is a periodic function of the variable y of zero average on Ω_{f}. Then, replacing expression (36) in Eq. (34), according to boundary conditions (35), we obtain the boundary value problem characterizing χ:

$$\begin{cases} \text{div}_y\left(D_k\left(I + \overline{\dfrac{\partial \chi}{\partial y}}\right)\right) = 0 \quad \text{in} \quad \Omega_{\text{f}} \\ D_k\left(I + \dfrac{\partial \chi}{\partial y}\right) \cdot n = 0 \quad \text{on} \quad \Gamma_{\text{sf}} \end{cases} \tag{37}$$

where I denotes the identity of $\mathbb{R}^3$.

(iv) *The macroscopic diffusion–migration model*

[5] The problem $\mathscr{P}_0$ is trivially satisfied according to (18).

According to the previous results, problem $\mathscr{P}_2$ reduces to

$$\begin{aligned}&\frac{\partial C_k^0}{\partial t} - \mathrm{div}_x\left(D_k\left(\frac{\partial C_k^0}{\partial x} + \frac{\partial C_k^1}{\partial y}\right) + D_k\left(\frac{\partial \Psi^0}{\partial x} + \frac{\partial \Psi^1}{\partial y}\right) Z_k C_k^0\right)\\ &-\mathrm{div}_y\left(D_k\left(\frac{\partial C_k^1}{\partial x} + \frac{\partial C_k^2}{\partial y}\right)\right) - \mathrm{div}_y\left(D_k\left(\frac{\partial \Psi^1}{\partial x} + \frac{\partial \Psi^2}{\partial y}\right) Z_k C_k^0\right)\\ &-\mathrm{div}_y\left(D_k\left(\frac{\partial \Psi^0}{\partial x} + \frac{\partial \Psi^1}{\partial y}\right) Z_k C_k^1\right) = 0 \text{ in } \Omega_\mathrm{f}\end{aligned} \tag{38}$$

The associated boundary conditions write

$$\begin{aligned}&\left(D_k\left(\frac{\partial C_k^1}{\partial x} + \frac{\partial C_k^2}{\partial y}\right) + D_k\left(\frac{\partial \Psi^1}{\partial x} + \frac{\partial \Psi^2}{\partial y}\right) Z_k C_k^0\right.\\ &\left.D_k\left(\frac{\partial \Psi^0}{\partial x} + \frac{\partial \Psi^1}{\partial y}\right) Z_k C_k^1\right) \cdot n = 0 \text{ on } \Gamma_\mathrm{sf}\end{aligned} \tag{39}$$

The integration of the Eq. (38) on the fluid domain Ω_f leads to

$$|\Omega_\mathrm{f}|\frac{\partial C_k^0}{\partial t} - \int_{\Omega_\mathrm{f}} \mathrm{div}_x\left(D_k\left(\frac{\partial C_k^0}{\partial x} + \frac{\partial C_k^1}{\partial y}\right) + D_k\left(\frac{\partial \Psi^0}{\partial x} + \frac{\partial \Psi^1}{\partial y}\right) Z_k C_k^0\right)\mathrm{d}\Omega = 0 \text{ in } \Omega_\mathrm{f}$$

where we have used the divergence theorem, the boundary conditions (39), and the periodicity conditions on Γ_ff to simplify the result.

To finish, let us replace $C_k^1 + \Psi^1 Z_k C_k^0$ by its expression (36) in the previous equation. We obtain the macroscopic diffusion–migration model of result 1:

$$\varphi\frac{\partial C_k^0}{\partial t} - \mathrm{div}_x\left(\mathbf{D_k^{hom}}\frac{\partial C_k^0}{\partial x} + \mathbf{D_k^{hom}}\frac{\partial \Psi^0}{\partial x} Z_k C_k^0\right) = 0$$

where the homogenized diffusion tensor $\mathbf{D_k^{hom}}$ is given by

$$\mathbf{D_k^{hom}} = \frac{1}{|\Omega|}\int_{\Omega_\mathrm{f}} D_k\left(I + \overline{\frac{\partial \chi}{\partial y}}\right)\mathrm{d}\Omega$$

and where χ is the solution of the boundary value problem (23).

4.3 Back to Dimensional Variables

To go back to the initial dimensional variables, let us define

$$C_k^{*0} = C_\mathrm{r} C_k^0, \quad \psi^{*0} = \psi_\mathrm{r}\psi^0, \quad D_k^{*\mathrm{hom}} = D_\mathrm{r} D_k^{\mathrm{hom}}, \quad \chi^* = l\chi \tag{40}$$

We then have the following result:

Result 2 *For orders of the dimensionless numbers such as* $\mathscr{R} = O(1)$, $\mathscr{A} = O(\varepsilon^2)$, $\tau = O(\varepsilon^2)$, $\mathscr{P} = O(\varepsilon^2)$, *the leading terms* C_k^{*0} *satisfy the electroneutrality assumption at the first order*:

$$\rho^{*0} = \sum_{k=1}^{N} Z_k C_k^{*0} = 0 \tag{41}$$

Moreover, the macroscopic concentration C_k^{*0} *and potential* Ψ^{*0} *at the scale of the material are solutions of the dimensional homogenized diffusion–migration model*:

$$\varphi \frac{\partial C_k^{*0}}{\partial t^*} - \mathrm{div}_{x^*}\left(\mathbf{D}_{\mathbf{k}}^{*\mathbf{hom}} \frac{\partial^* C_k^{*0}}{\partial x^*} + \frac{F Z_k}{RT} \mathbf{D}_{\mathbf{k}}^{*\mathbf{hom}} \frac{\partial^* \Psi^{*0}}{\partial x^*} C_k^{*0}\right) = 0 \tag{42}$$

The homogenized dimensional diffusion tensor $\mathbf{D}_{\mathbf{k}}^{*\mathbf{hom}}$ *is given by*:

$$\mathbf{D}_{\mathbf{k}}^{*\mathbf{hom}} = \frac{1}{|\Omega^*|} \int\limits_{\Omega_{\mathrm{f}}^*} D_k^* \left(I + \overline{\frac{\partial^* \chi^*}{\partial y^*}}\right) \mathrm{d}\Omega^* \tag{43}$$

where the vector $\chi^*(y^*)$ *is the solution of the boundary problem*:

$$\begin{cases} \mathrm{div}_{y^*}\left(D_k^*\left(I + \overline{\frac{\partial^* \chi^*}{\partial y^*}}\right)\right) = 0 \text{ in } \Omega_{\mathrm{f}^*} \\ D_k^*\left(I + \frac{\partial^* \chi^*}{\partial y^*}\right) \cdot n = 0 \text{ on } \Gamma_{\mathrm{sf}}^* \end{cases} \tag{44}$$

Proof Let us go back to the physical variables (40) in equations of result 1. It stands

$$\frac{\varphi t_{\mathrm{r}}}{C_{\mathrm{r}}} \varphi \frac{\partial C_k^{*0}}{\partial t^*} - \mathrm{div}_{x^*}\left(\frac{L^2}{C_{\mathrm{r}} D_{\mathrm{r}}} \mathbf{D}_{\mathbf{k}}^{*\mathbf{hom}} \frac{\partial^* C_k^{*0}}{\partial x^*} + \frac{L^2}{D_{\mathrm{r}} \psi_{\mathrm{r}} C_{\mathrm{r}}} Z_k \mathbf{D}_{\mathbf{k}}^{*\mathbf{hom}} \frac{\partial^* \Psi^{*0}}{\partial x^*} C_k^{*0}\right) = 0$$

or equivalently

$$\frac{\varphi \varepsilon^2}{\tau} \frac{\partial C_k^{*0}}{\partial t^*} - \mathrm{div}_{x^*}\left(\mathbf{D}_{\mathbf{k}}^{*\mathbf{hom}} \frac{\partial^* C_k^{*0}}{\partial x^*} + \frac{1}{\mathscr{R}} \frac{F Z_k}{RT} D_k^{*\mathrm{hom}} \frac{\partial^* \Psi^{*0}}{\partial x^*} C_k^{*0}\right) = 0$$

Then using the order of magnitude of the dimensionless numbers given by (13), we have $\tau = O(\varepsilon^2)$ and $\mathscr{R} = O(1)$, which leads to the dimensional equation (42). The end of the proof of the result does not contain any difficulty and is left to the reader. □

5 Experimental Study

In this experimental study, two cement pastes were submitted to electrodiffusion test by applying an external electrical field to accelerate the transport process (Amiri et al. 1997). In addition of the microstructure parameters given by the literature (Aït-Mokhtar et al. 1999, 2004) some other parameters involved in this experimental study served in parallel for the boundary conditions used in the simulations carried out in the sections below.

5.1 Materials

Prismatic specimens (12 × 12 × 20) cm of two cement pastes (with two water/cement w/c ratios: 0.5 and 0.7) were manufactured without any workability agent. The cement used is of type CEM I 52.5 (according to European standards EN 197-1) with the chemical composition given in Table 1. In order to avoid leaching phenomena, the specimens have been cured, just after being turned, during 28 days in an alkaline solution, which is closed to the natural interstitial solution of cement-based materials, namely 83 mol m^{-3} KOH, and 25 mol m^{-3} NaOH (Amiri et al. 2001a,b; Friedmann et al. 2004, 2008).

Table 1 Chemical composition of cement used

Oxides	CaO	SiO_2	Al_2O_3	Fe_2O_3	MgO	K_2O
Composition (wt%)	64.02	19.81	5.19	2.38	0.9	1.11
Oxides	Na_2O	SO_3	TiO_2	MnO	SiO	P_2O_5
Composition (wt%)	0.06	3.5	0.28	0.05	0.15	0.16

Table 2 Characteristics of the tested cement pastes

Type of cement paste	w/c	Porosity Hg (%)
Paste 1	0.5	18
Paste 2	0.7	29

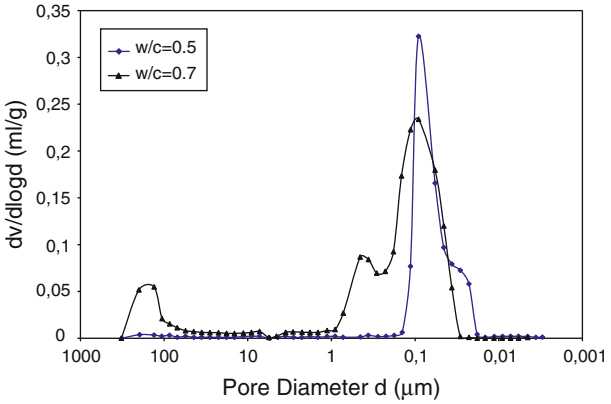

Fig. 2 Pore size distributions of the cement pastes obtained by MIP

5.2 Porosimetry Tests

The porosities and the pore size distribution of the cement pastes were measured by the MIP. Samples were appropriated from the heart of the prismatic specimens and then dried during 24 h at 70°C. Mercury injection measurements were done with Micromeritics porosimeter (Autopore III 9420) the range of pressure of which reaches more than 400 MPa. This pressure allows the mercury to penetrate pores of 3 nm of diameter approximately, according to Laplace law:

$$d = \frac{-4\sigma \cos\theta}{p}$$

where d is the equivalent diameter of the intruded pores, σ the surface tension of mercury ($0.485\,\mathrm{Nm}^{-1}$), θ the contact angle between mercury and the pore walls system (130°), and p is the pressure at which a given increment of mercury intrudes the pores (Aït-Mokhtar et al. 1999, 2004).

The values of the obtained porosities and of the pore size distributions are shown, respectively, in Table 2 and in Fig. 2.

Figure 2 shows that paste 1 (with $w/c = 0.5$) presents mono-modal distribution corresponding to capillary porosity. On the other hand, the paste 2 (with $w/c = 0.7$) presents a tri-modal distribution corresponding to weak micro porosity and a large capillary porosity.

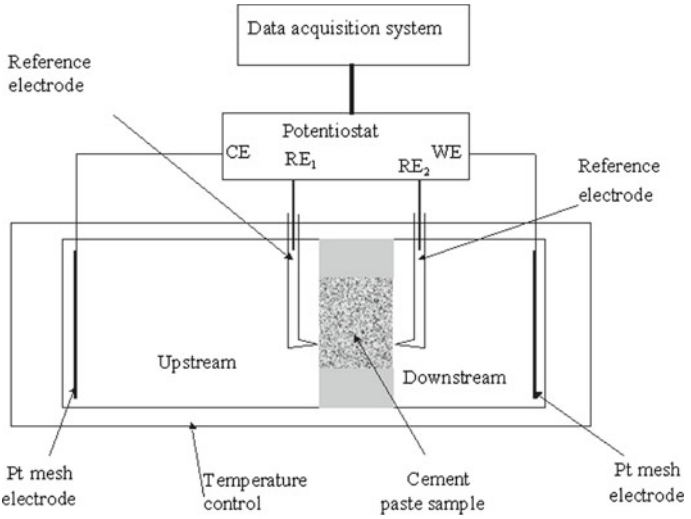

Fig. 3 Experimental device used for electrodiffusion tests

In addition of the capillary porosity, this distribution highlights a larger pore diameter, respectively around 0.6 and 200 μm, approximately.

5.3 Electrodiffusion Test

Samples tested in electrodiffusion were obtained by a technique of core sampling and cutting to a disk measuring 6.5 cm in diameter and 1 cm in thickness. This kind of samples allows avoiding wall effects, classically encountered in cementitious materials. The lateral surface was covered with a resin to insure a unidirectional transfer. The experimental setup is depicted in Fig. 3. The sample is placed between two compartments. The upstream one is of 2 l volume, while the downstream one is 1 l, so as it allows detecting earlier chlorides by dosage in this downstream compartment. A voltage is applied between two platine electrodes using a potentiostat with a four electrode device. The two other electrodes are reference electrodes used to monitor a constant electrical field accurately (300 V m^{-1}) between the opposite faces of the sample. The concentrations of NaOH and KOH are the same as those used for the cure described in Sect. 5.1. In a first step, the electrical field is applied to the cell containing the same basic solution of KOH and NaOH in upstream and downstream compartments. After reaching a first steady state regime, 500 mol m^{-3} concentration of NaCl was added to the upstream and, once again, the electrical field is applied. Then, chlorides migrate through the sample toward the downstream. The chloride concentration is measured in the downstream by potentiometric titration until obtaining a constant chloride flux corresponding to the steady state (see Fig. 4). The titration method consists in comparing the measured potential between two electrodes in a solution of unknown chloride concentration (selective electrode) with potential measured in a solution of known chloride concentration (working electrode). The two electrodes are connected to a millivoltmeter. After each dosage, the two compartment solutions are renewed with respect to the boundary conditions: a constant chlorides concentration at the upstream (500 mol m^{-3}) and no chlorides at the downstream.

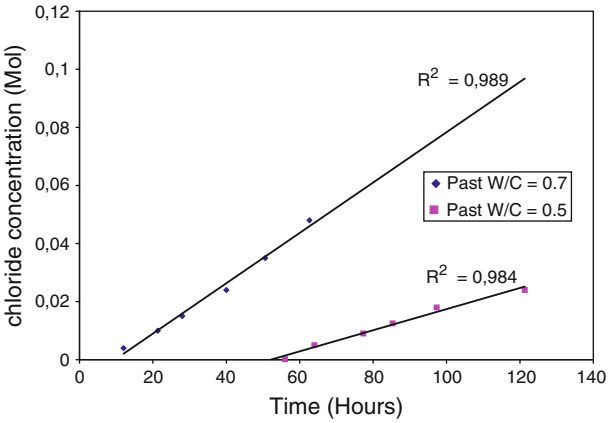

Fig. 4 Evolution of the cumulated chlorides concentration in the downstream compartment according to time

5.4 Results

The evolution of cumulated chloride concentration according to time, in the downstream compartment is given in Fig. 4. The gradient of the linear part of the curve gives the constant flux at the steady state:

$$J^* = \frac{\Delta C^*_{\mathrm{Cl}^-} V_{\mathrm{a}^*}}{\Delta t^* A^*} \tag{45}$$

where V_{a^*} is the volume of the downstream compartment of the cell, A^* is the sample surface submitted to ionic transfer and $\Delta C^*_{\mathrm{Cl}^-}$ is the variation of the chloride concentration measured during a period of time Δt^*.

The determination of the experimental macroscopic diffusion coefficient is given by the available literature (Amiri et al. 2001b) which shows that it can be expressed as:

$$D^{*\mathrm{exp}}_{\mathrm{Cl}^-} = \frac{RTJ^*}{Z_{\mathrm{Cl}^-} F \| E^{*0} \| C^*_0} \left(1 - \exp\left(-\frac{Z_{\mathrm{Cl}^-} F}{RT} U_{\mathrm{e}}\right)\right) \tag{46}$$

where C^*_0 denotes the initial chloride concentration in the upstream compartment, U_{e} the potential difference applied over the sample's length L. Note that literature highlights that the macroscopic diffusion coefficient is the same whatever the value of the accelerated electrical field, i.e., migration or natural diffusion.

For the two cement pastes considered, the measured chloride flux J^* and the value of the diffusion coefficient $D^{*\mathrm{exp}}_{\mathrm{Cl}^-}$ are obtained from the numerical application of Eq. (46). They are summarized in Table 3.

Table 3 Values of flux and diffusion coefficient obtained for the two cement pastes tested

Type of cement paste	w/c = 0.5	w/c = 0.7
J^* (mol m^{-2} s^{-1})	3.42×10^{-5}	7.72×10^{-5}
$D^{*\mathrm{exp}}_{\mathrm{Cl}^-}$ (m^2 s^{-1})	5.95×10^{-12}	13.40×10^{-12}

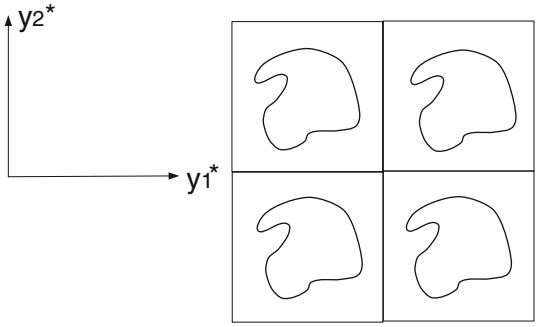

Fig. 5 Periodic microstructure with cylindrical pores

6 Simple Cylindrical Pore Model

6.1 Analytical Solution for Cylindrical Pore Geometry

Let us consider the simple case of a porous material the microstructure of which is constituted of cylindrical pores[6], where the direction y_3^* is that of the axis of the pores (Fig. 5). In that case, we can exhibit an analytical solution $\chi^*(y^*)$ of problem (47). It is generally not the case as soon as the microstructure is more complex.

For sake of simplicity, we consider that the transfer in the fluid phase is isotropic, and that the diffusion coefficient D_k^* is constant. The expression of $\mathbf{D}_\mathbf{k}^{*\mathbf{hom}}$ becomes

$$\mathbf{D}_\mathbf{k}^{*\mathbf{hom}} = \frac{D_k^*}{|\Omega^*|} \int\limits_{\Omega_{\mathrm{f}^*}} \left(I + \overline{\frac{\partial^* \chi^*}{\partial y^*}} \right) \mathrm{d}\Omega^*$$

where the vector $\chi^*(y)$ is solution of the Neumann problem:

$$\begin{cases} \Delta_{y^*} \chi^* = 0 \quad \text{in} \quad \Omega_{\mathrm{f}^*} \\ \dfrac{\partial \chi^*}{\partial y^*} \cdot n = -n \quad \text{on} \quad \Gamma_{\mathrm{sf}}^* \end{cases} \tag{47}$$

The periodical condition of χ^* on the cell boundary Γ_{ff}^* is automatically satisfied (because of the geometry of the cell). According to the geometry of the problem, we search a solution $\chi^*(y_1^*,\ y_2^*)$ not depending on the variable y_3^*, the components χ_i^* of which are solution of

$$\Delta_{y^*} \chi_i^* = 0 \text{ in } \Omega_{\mathrm{f}^*} \quad \text{for } i = 1,\ 2,\ 3$$

with the associated boundary conditions

$$\begin{aligned} \left(\frac{\partial \chi_1^*}{\partial y_1^*} + 1 \right) n_1 + \frac{\partial \chi_1^*}{\partial y_2^*} n_2 &= 0 \quad \text{on} \quad \Gamma_{\mathrm{sf}}^* \\ \frac{\partial \chi_2^*}{\partial y_1^*} n_1 + \left(\frac{\partial \chi_2^*}{\partial y_2^*} + 1 \right) n_2 &= 0 \quad \text{on} \quad \Gamma_{\mathrm{sf}}^* \\ \frac{\partial \chi_3^*}{\partial y_1^*} n_1 + \frac{\partial \chi_3^*}{\partial y_2^*} n_2 &= 0 \quad \text{on} \quad \Gamma_{\mathrm{sf}}^* \end{aligned}$$

[6] We recall that in the mathematical sense, a cylinder is constituted of generators which lean against any closed curve (the shape of the cylinder).

It is clear that the solution of this problem writes

$$\begin{aligned}\chi_1^*(y_1^*,\ y_2^*) &= -y_1^* + a\\ \chi_2^*(y_1^*,\ y_2^*) &= -y_2^* + b\\ \chi_3^*(y_1^*,\ y_2^*) &= c\end{aligned}$$

where $a,\ b,\ c$ are the arbitrary constants[7] which can be determined by a zero average condition for χ^* on Ω_{f^*}. However, they do not influence the value of $\mathbf{D}_{\mathbf{k}}^{*\mathbf{hom}}$ the computation of which leads to

$$\mathbf{D}_{\mathbf{k}}^{*\mathbf{hom}} = \varphi D_k^* \begin{pmatrix} 0 & 0 & 0 \\ 0 & 0 & 0 \\ 0 & 0 & 1 \end{pmatrix} \tag{48}$$

where we recall that $\varphi = \frac{|\Omega_f^*|}{|\Omega^*|}$ denotes the porosity of the material. This result is here established, in general, for any cylindrical pores. Thus, whatever the cylinder shape is (not necessary circular), we always obtain the same value of the homogenized tensor $\mathbf{D}_{\mathbf{k}}^{*\mathbf{hom}}$ given by (48).

6.2 Comparison with Experimental Results

For the cement pastes considered experimentally in Sect. 5, their respective porosities is given in Table 2. The application of formula (48) leads to a value of the homogenized chlorides coefficient $D_{\mathrm{Cl}^-}^{*\mathrm{hom}}$ which is far from the experimental one given in Table 3. This difference can be attributed in particular to

(i) a too simple geometric description of the microstructure with the cylindrical pore model considered. In reality, the pores have a complex geometry with mainly a tortuosity and constrictivity. These parameters influence the materials' diffusivity; they contribute to slow down the transfer.

(ii) the neglecting of the adsorption phenomena which occur at the interface between the solid phase and the liquid one within the material called electrical double layer (Amiri et al. 2001b). They can have a strong effect on the ionic transfer in pores with small sizes. In what follows, we will focus on point (i) and consider more complex geometric models for the elementary cell, leading to a larger tortuosity and constrictivity.

7 Numerical Resolution for More Complex Cell Geometries

We consider in this section a more complex material microstructure through a more complex cell geometry, and compute the corresponding homogenized diffusion tensor $\mathbf{D}_{\mathbf{k}}^{*\mathbf{hom}}$. In those cases, analytical solutions of problem (47) do not exist and we will have recourse to numerical resolution and calculation of $\mathbf{D}_{\mathbf{k}}^{*\mathbf{hom}}$, first for a two-dimensional cell geometry and then for three-dimensional ones. In all the cases studied, we will consider to simplify the calculations that the diffusion coefficient $D_k^{*\mathrm{hom}}$ is constant so that the problem to solve reduces to problem (47) to determine the vector $\chi^*(y^*)$. An important point to quote is that

[7] We recall that the solution of Neumann problem (47) is defined up arbitrary constants.

the three components χ_i^* (for $i = 1,\ 2,\ 3$) of χ^* can be determined independently by solving:

$$\triangle_{y^*} \chi_i^* = 0 \quad \text{in} \quad \Omega_{\mathrm{f}^*} \tag{49}$$

$$\frac{\partial \chi_i^*}{\partial y^*} \cdot n = -n_i \quad \text{on} \quad \Gamma_{\mathrm{sf}}^* \tag{50}$$

$$\chi_i^* \quad \text{is periodic on } \Gamma_{\mathrm{ff}}^* \tag{51}$$

$$\langle \chi_i^* \rangle = 0 \quad i = 1, 2, 3 \tag{52}$$

where $\langle \chi_i^* \rangle$ denotes the average of χ_i^* on Ω^*. Once χ^* computed numerically, we calculate the homogenized diffusion tensor $\mathbf{D}_{\mathbf{k}}^{*\mathbf{hom}}$ as follows:

$$\begin{aligned} \mathbf{D}_{\mathbf{k}}^{*\mathbf{hom}} &= \frac{D_k^*}{|\Omega^*|} \int_{\Omega_{\mathrm{f}^*}} \left(I + \overline{\frac{\partial^* \chi^*}{\partial y^*}} \right) \mathrm{d}\Omega^* \\ &= \varphi D_k^* \left(I + \frac{1}{|\Omega_{\mathrm{f}}^*|} \int_{\Gamma_{\mathrm{sf}}^*} n \otimes \chi^* d\Gamma^* \right) \end{aligned} \tag{53}$$

using the divergence theorem and the periodicity condition on the boundary Γ_{ff}^*, where $\otimes$ denotes the tensorial product.

The numerical resolution of Neumann problem (49)–(52) is performed by the software Comsol Multiphysics ® based on the finite element method.

7.1 Two Dimensional Problem

Let us consider a porous medium the microstructure of which is composed of the periodical repetition of an elementary cell, itself composed of a disk located at the center of the cell, and of a quarter of disk of smaller radius located at each corner of the cell (Fig. 6a).

The size of the periodic cell is 1×1. The bigger disk, located at the center $(0.5,\ 0.5)$, has a radius $R = 0.45$. The quarters of disk have a varying radius $r \in [0.05,\ 0.255]$, leading to porosities of the material $\varphi \in [0.16,\ 0.37]$. The external boundaries (1–4) represent the fluid–fluid interface Γ_{ff}^* between cells, on which χ^* is imposed to be periodical for the resolution. The boundaries 5–9 represent the solid–fluid interface Γ_{sf}^* on which the boundary

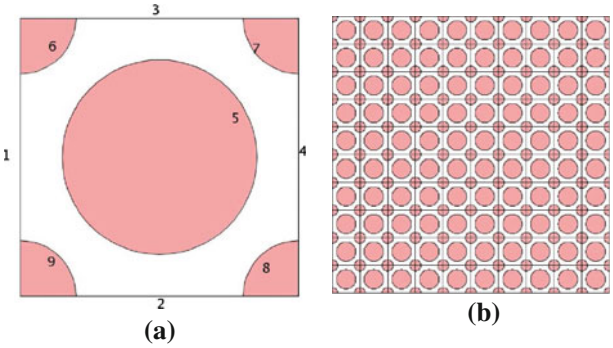

Fig. 6 A bi-circular inclusion model. **a** The elementary cell. **b** The material with the associated periodic microstructure

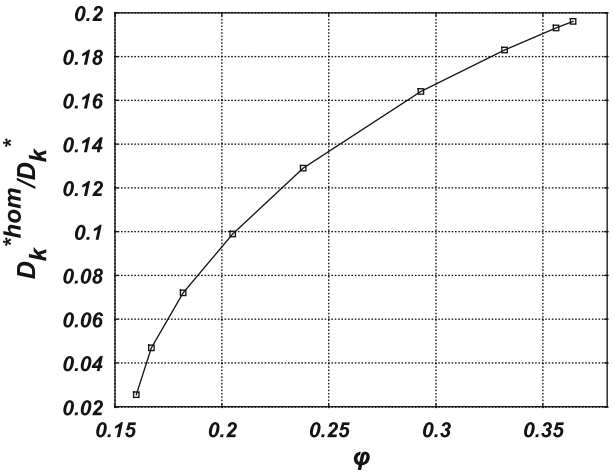

Fig. 7 Relative homogenized diffusion coefficient versus porosity for bi-circular inclusion model

conditions are imposed for χ^*. For various values of $r \in [0.05, 0.255]$, we solve numerically the Neumann problem (49)–(52) by Comsol Multiphysics®, for the elementary cell of Fig. 6a. Once $\chi^*(y^*)$ determined, we compute numerically the homogenized diffusion coefficient $D_k^{*\text{hom}}/D_k^*$ by (53) as previously. According to the geometry of the cell, it is isotropic. For various values of the porosity φ, we plot $D_k^{*\text{hom}}/D_k^*$ with respect to φ on Fig. 7. We observe a very strong decreasing of $D_k^{*\text{hom}}/D_k^*$ when the porosity becomes lower than 0.25. With this geometry of the elementary cell, we can attempt weak porosities close to the experimental values of the cement pastes considered in Sect. 5. Thus, the comparison with the experimental values of Table 3 of $D_{\text{Cl}^-}^{*\text{exp}}$ is relevant. For a porosity $\varphi = 0.18$, modeled with such a geometry of the elementary cell, we find that $D_{\text{Cl}^-}^{*\text{hom}} = 8 \times 10^{-11}\,\text{m}^2/\text{s}$. This value is 12 times larger than the experimental one $D_{\text{Cl}^-}^{*\text{exp}} = 5.95 \times 10^{-12}\,\text{m}^2/\text{s}$ obtained in Table 3 for the cement paste which has the same porosity (see Table 2). The same ratio of the theoretical value to the experimental one of $D_{\text{Cl}^-}^{*\text{hom}}$ is obtained for the cement paste 2 considered. However, the result being strongly dependent on the topology of the porous network of the elementary cell, we will consider in the next section three-dimensional geometries closer to the real microstructure.

7.2 Three-Dimensional Problems

The problem to solve is still the Neumann problem (49)–(52), where the domain Ω_{f^*} is now three-dimensional so that the unknown function χ^* depends on y_1^*, y_2^* and y_3^*. In all the cases considered, according to the symmetries of the cells, the homogenized diffusion tensor will be isotropic (spherical) so that only the diffusion coefficient $D_k^{*\text{hom}}$ will be computed numerically, as previously for 2D problems.

Let us consider a complex 3D elementary cell (similar to that considered in 2D) composed of a sphere of varying radius $R \in [0.2,\ 0.475]$ located at the center, and of 1/8th of spheres of radius r varying in $[0.1,\ 0.375]$ located at the corners of the cell. The variation of $r \in [0.1,\ 0.375]$ implies a variation of the porosity $\varphi \in [0.33, 0.962]$. The surface of the inclusions represents the solid–fluid interface Γ_{sf}^*, where the boundary conditions (50) are imposed. Periodic conditions for χ^* are imposed on the external boundary of the cell. The

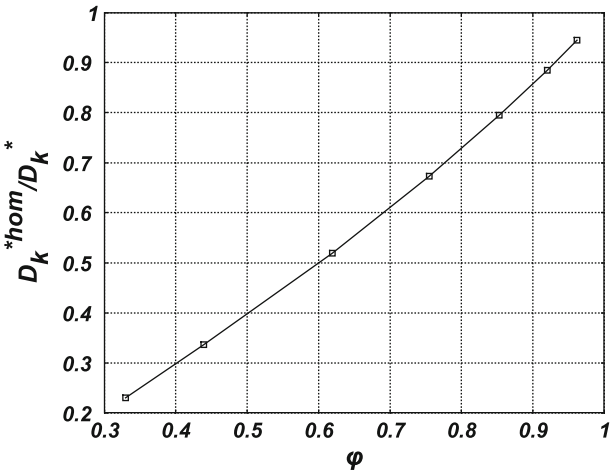

Fig. 8 Variation of the relative homogenized diffusion coefficient $D_{\mathrm{k}}^{*\mathrm{hom}}/D_{\mathrm{k}*}$ versus the porosity

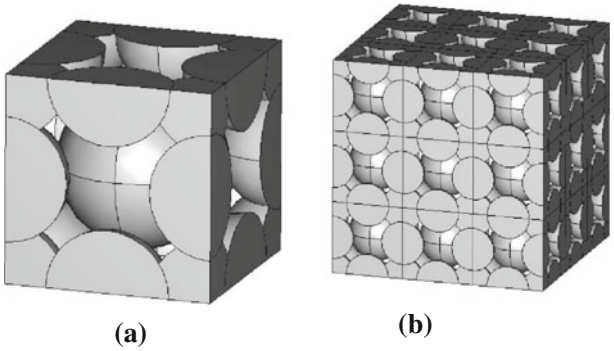

Fig. 9 Complex inclusion by octahedric distribution of two types of spherical inclusions. **a** Elementary cell. **b** The associated material with periodic microstructure

mesh used for the 3D numerical resolution by Comsol Multiphysics is composed of Lagrange quadratic tetrahedral elements in $\Omega_{\mathrm{f}*}$ and triangular elements on the boundaries.

In Fig. 8, the variation of $D_k^{*\mathrm{hom}}/D_k^*$ is plotted with respect to the porosity φ. We observe a decrease of $D_k^{*\mathrm{hom}}/D_k^*$ when φ decreases. However, unlike the two-dimensional case, we cannot here attempt porosities close to 0.18 corresponding to the cement pastes studied. With the 3D cell considered here, we are limited to porosities close to 0.3. This is due to the very different topology of the porous network in 2D and in 3D. Therefore, to attempt lower porosities (lower than $\varphi = 0.20$), we will consider a last more complex elementary cell (Fig. 9a). It is composed of the same previous elementary cell of Fig. 10a, to which we added 1/4th of spheres of the same varying radius r located on each side of the cell. The size of the bigger sphere located at the center does not vary. Only the radius r of the 1/4th and 1/8th of spheres varies in the interval $[0.2,\ 0.7]$. During this increase of size, the sphere located on each side of the elementary cell are allowed to interpenetrate those at the corners.[8] With this elementary cell, for r varying in the interval $[0.2,\ 0.7]$, we have $\varphi \in [0.09,\ 0.60]$

[8] This penetration could be representative of the hydration process of the cement pastes.

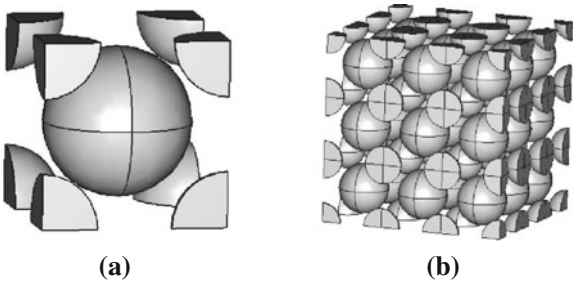

Fig. 10 The periodic medium with elementary cell with two types of spherical inclusions. **a** Elementary cell containing two types of spherical inclusions (solid phase). **b** Associated material with periodic microstructure

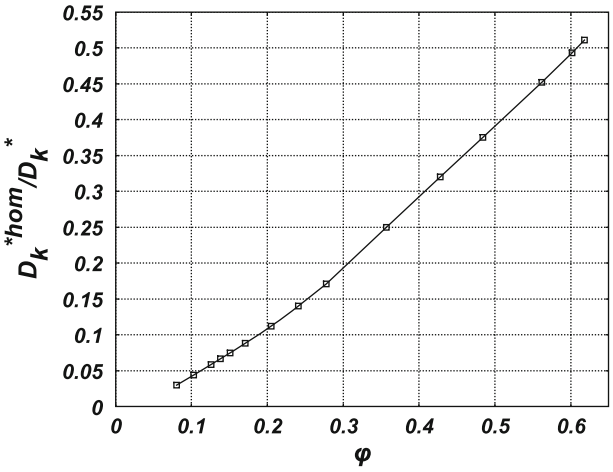

Fig. 11 Relative homogenized diffusion coefficient as function of porosity

and we can attempt weak porosities. The variation of the relative homogenized diffusion coefficient $D_k^{*\mathrm{hom}}/D_k^*$ with respect to φ is plotted on Fig. 11. We observe a slow decrease of $D_k^{*\mathrm{hom}}/D_k^*$ when φ decreases, even for very weak porosities. Once again in 3D, we do not observe a strong decrease of the homogenized diffusion coefficient for φ around 0.15. That was a particularity of the 2D cell considered in Fig. 6a, for dense circular inclusions, when the 2D disks were very closed together, leading to a very weak percolation between inclusions.

8 Conclusion

This study highlights the relevance of the use of the periodic homogenization technique for studying ionic transport in saturated porous materials. The heterogeneity of the material is taken into account by a periodic distribution of an elementary cell. The dimensional analysis of Nernst–Planck equation allows characterizing the problem through some dimensionless numbers. For a weak applied electrical field, we obtained a macroscopic model coupling diffusion and migration. The expression of the homogenized diffusion tensor only involves the geometrical properties of the material microstructure.

We proposed in the second part of this paper, analytical (when it was possible) and numerical calculations of the homogenized diffusion tensor $\mathbf{D}_\mathbf{k}^{*\mathbf{hom}}$ for various 2D and 3D cell

geometries leading to gradual complexities of the periodical porous network. All the homogenized diffusion coefficients computed numerically, in particular for complex three-dimensional cells, do not allow getting values close to the experimental ones, which are quite weaker. These results highlight that the chemical and electrocapillary adsorption phenomena (or electrical double layer effect) cannot be neglected for ionic diffusion in cementitious materials. It contributes to slow down the ionic transfer, particularly in pores of small diameters (nanopores), even more than a complex tortuosity and constrictivity of the porous network. Moreover, the multi-scale character of cementitious materials, containing porosities at very different scales, must be taken into account as well.

References

Aït-Mokhtar, A., Amiri, O., Sammartino, S.: Analytic modeling and experimental study of the porosity and the permeability of porous media, application to cement mortars and granitic rocks. Mag. Concr. Res. **51**, 391–396 (1999)

Aït-Mokhtar, A., Amiri, O., Dumargue, P., Bouguerra, A.: On the applicability of Washburn law: study of mercury and water flow properties in cement-based materials. Mater. Struct. **37**, 107–113 (2004)

Amiri, O., Aït-Mokhtar, A., Seigneurin, A.: A complement to the discussion of A. Xu and S. Chandra, about the paper "Calculation of chloride coefficient diffusion in concrete from ionic migration measurements" by C. Andrade. Cem. Concr. Res. **27**, 951–957 (1997)

Amiri, O., Aït-Mokhtar, A., Dumargue, P., Touchard, G.: Electrochemical modelling of chloride migration in cement based materials. Part I: theoretical basis at microscopic scale. Electrochim. Acta. **46**, 1267–1275 (2001a)

Amiri, O., Aït-Mokhtar, A., Dumargue, P., Touchard, G.: Electrochemical modelling of chlorides migration in cement based materials. Part II: experimental study—calculation of chlorides flux. Electrochim. Acta. **46**, 3589–3597 (2001b)

Auriault, J.L., Lewandowska, J.: Diffusion/adsorption/advection macrotransport in soils. Eur. J. Mech. A. **15**(4), 681–704 (1996)

Auriault, J.L., Lewandowska, J.: Diffusion non-linaire en milieux poreux. C. R. Acad. Sci. **324**, 293–298 (1997)

Auriault, J.L., Strzelecki, T.: On the electro-osmotic flow in a saturated porous. Int. J. Eng. Sci. **19**(7), 915–928 (1981)

Baltean, D., Levy, T., Balint, S.: Diffusion–convection in a porous medium with imprevious inclusions at low rates. Transp. Porous Media **51**, 19–39 (2003)

Bard, A.-J., Faulkner, L-R.: Electrochemical Methods. Fundamentals and Applications. 2nd edn. Wiley, New York (2001)

Bensoussan, A., Lions, J.L., Papanicolaou, G.: Asymptotic analysis for periodic structures. In: Lions, J.L., Papanicolaou, G., Rockafellar, R.T. (eds.) Studies in Mathematics and its Applications (1978)

Friedmann, H., Amiri, O., Aït-Mokhtar, A., Dumargue, P.: A direct method for determining chloride diffusion coefficient by using migration test. Cem. Concr. Res. **34**, 1967–1973 (2004)

Friedmann, H., Amiri, O., Aït-Mokhtar, A.: Shortcomings of geometrical approach in multi-species modelling of chloride migration in cement-based materials. Mag. Concr. Res. **60**, 119–124 (2008)

Hamdouni, A., Millet, O.: Classification of thin shell models deduced from the nonlinear three-dimensional elasticity. Part I: the shallow shells. Arch. Mech. **55**(2), 135–175 (2003)

Klinghoffer, O., Frolund, T., Poulsen, E.: Rebar corrosion rate measurements for service life estimates. ACI Fall Convention 2000, Toronto, Canada, Committe 365 "Practical Application of Service Life Models"

Lipkowski, J., Ross, P.-N.: Electrochemistry of Novel Materials. Wiley-VCH Edition, New York (1994)

Millet, O., Hamdouni, A., Cimetière, A.: Justification du modèle bidimensionnel non linéaire de plaque par développement asymptotique des équations d'équilibre. C. R. Acad. Sci. Paris **324**, 349–354 (1997)

Millet, O., Hamdouni, A., Cimetière, A.: A classification of thin plate models by asymptotic expansion of nonlinear three-dimensional equilibrium equations. Int. J. Non-Linear Mech. **36**, 165–186 (2001)

Millet, O., Aït-Mokhtar, A., Amiri, O.: Determination of the macroscopic chloride diffusivity in cementitious porous materials by coupling periodic homogenization of Nernst–Planck equation with experimental protocol. Int. J. Multiphys. **2**(1), 129–145 (2008)

Moyne, C., Murad, M.: Macroscopic behavior of swelling porous media derived from micromechanical analysis. Transp. Porous Media **50**, 127–151 (2003)

Moyne, C., Murad, M.: A two-scale model for coupled electro-chemo-mechanical phenomena and onsager's reciprocity relations in expansive clays: I homogenization analysis. Transp. Porous Media **62**, 333–380 (2006)

Newman, J., Thomas-Alyea, K.E.: Electrochemical Systems. 3rd edn. Wiley, Hoboken (2004)

Poupard, O., Aït-Mokhtar, A., Dumargue, P.: Impedance spectroscopy in reinforced concrete: procedure for monitoring steel corrosion: Part I development of the experimental device. J. Mater. Sci. **38**, 2845–2850 (2003a)

Poupard, O., Aït-Mokhtar, A., Dumargue, P.: Impedance spectroscopy in reinforced concrete: experimental procedure for monitoring steel corrosion: Part II polarization effect. J. Mater. Sci. **38**, 3521–3526 (2003b)

Quintard, M., Whitaker, S.: Transport in ordered and disordered porous media: the cellular average and use of weighting function. Transp. Porous Media **14**(2), 163–177 (1994)

Samson, E., Marchand, J., Beaudoin, J.J.: Describing ion diffusion mechanisms in cement-based materials using the homogenization technique. Cem. Concr. Res. **29**(8), 1341–1345 (1999)

Sanchez Palencia, E.: Non-homogeneous Media and Vibration Theory. Lecture Notes in Physics. Springer, New York (1980)

Skjetne, E., Auriault, J.L.: New insights on steady, non-linear flow in porous media. Eur. J. Mech. B. **18**(1), 131–145 (1999)

Whitaker, S.: Diffusion and reaction in a micropore–macropore model of a porous medium. Lat. Am. J. Appl. Chem. Eng. **13**, 143–183 (1983)

Whitaker, S., Plumb, A.O.: Dispersion in heterogeneous porous media, 1 local volume averaging and large-scale averaging. Water Resour. Res. **24**, 913–926 (1988)